proach for spacecraft radars. Some years ago in a brilliant concept, it was observed that coherence should obtain for two separate passes of a single space-borne radar if the two orbits were sufficiently close together (*3*). The technique has been demonstrated repeatedly for the derivation of terrain height profiles, for which an orbital separation on the order of a kilometer is typical. For observation of displacements in the scene, such as vertical or horizontal motion between the two radar observations, the two orbits should be nearly identical.

Coherence of the radar is necessary, but not sufficient, for interferometry. There also are conditions on both the viewing geometry and the scene reflectivity. The two reflected fields must be such that they are mutually coherent. Even when the viewing geometry may be identical, if the backscattered field is different on the two opportunities, then the relative phase structure between the two (complex) data files is random, and no fringes can result. It follows that there are both spatial and temporal constraints on the orbit opportunities for SAR interferometric data collection.

Spatially, the two orbital passes must follow the same nominal trajectory. Available opportunities are set by the mission repeat cycle, which is the number of orbits, or days, required for the satellite to begin retracing its Earth footprint (*4*). Even for pairs of orbits having the same nominal Earth track, the two satellite trajectories may differ by many kilometers. The actual difference depends on many factors, including orbital decay, spacecraft repositioning strategies, and so forth. The orbits reported in (*2*) had only 4-m spacing, the most favorable pair among the set available.

For all situations involving a dynamic medium such as ice, mutual coherence between two data sets decreases with increasing observation time interval. The intervals of opportunity are determined by the orbit repeat cycle. For example, Earth Remote Sensing Satellite-1 (ERS-1) used a 3-day repeat cycle during the commissioning phase and again for a few weeks during a later phase, but a 35-day cycle is more typical of its operational life. Cycles less than about 25 days do not allow complete global coverage for satellites with an imaging swath width of only 100 km, so there is pressure from most users to avoid shorter periodicity. Even with a relatively short interval such as 3 days, if there is temperature change or precipitation in the meantime, then coherence sufficient for useful fringes may not be sustained. It follows that short repeat cycles are preferred for interferometry and that several opportunities should be available for each interferometric pair desired. Moreover, the coherence image (fringe contrast) may be interpreted as a mapping of the degree of change in the reflectivity process, which is complementary to the fringes themselves, whose spacing is proportional to the gradient of bulk movement of the scatterers. Goldstein *et al.* (*2*) apply interferometric motion measurement to the Rutford Ice Stream, one of the main outlets of the West Antarctic ice sheet. Such flows, with rates on the order of 0.5 km/year, account for about 90% of the outflow from the sheet. Details of flow dynamics are difficult if not impossible to observe using standard techniques. The interferometric estimates reported by Goldstein *et al.* are sensitive to differential motions of a millimeter per day, mapped simultaneously over the ice flow width approaching 100 km. Estimates over the area of the sheet derived from interferometry compare favorably with data from in situ observations. Quantitative monitoring of the Rutford Ice Stream and similar phenomena is one means of anticipating significant changes in the Arctic ice environment, linked inextricably to the Earth's environment.

Fahnestock *et al.* (*1*) use radar images from many orbital opportunities to assemble a mosaic of the ice cover of Greenland. Beyond the usual radar advantages of imagery through cloud and darkness, microwave penetration allows observation of changes within the ice sheet. Ice sheet regimes, as well as their seasonal or regional changes, may be mapped. Unlike the interferometric method, which is limited to estimation of motion components only in the direction toward the radar, the observations by Fahnestock *et al.* show changes on a near-continental scale independent of radar vantage point. A significant ice stream is reported in the northeast of Greenland, having physical similarities to the Rutford Ice Stream. Flow rates on the order of 0.5 km/year are estimated using two sets of imagery taken one year apart, although details of differential flow structure are not readily observable. Both articles offer comments on the relative advantages and disadvantages of various satellite techniques for monitoring changes in ice sheets.

There are two imaging radar satellite systems now in Earth orbit and at least four more planned for operation during the next 10 years (*4*). All of these have high resolution (nominally 25 m or better) and are capable of routine and repeated observation of the Earth's ice distribution. From the standpoint of ice studies and global change, it would make sense to establish a set of test sites in both the Arctic and Antarctica for regular observation by these systems over many years. In principle, both the image registration technique and the space-borne radar interferometer technique may be used with these radars. However, none of them have been designed with interferometric capability as a mission requirement. With the exception of commissioning phases of certain systems, only the ERS-1 and ERS-2 radars include 3-day revisit cycles, from which they have access to only a fraction of the globe, and then only during the northern winter season. The value of these satellite radars would be enriched if short revisit intervals were adopted for a part of each mission so that interferometry, both in the polar regions and for other global applications, could be supported.

References and Notes

1 M Fahnestock *et al.*, *Science* **262**, 1530 (1993).
2 R M. Goldstein *et al.*, *ibid.*, p 1525.
3. A. K. Gabriel, R M. Goldstein, H. A. Zebker, *J. Geophys. Res.* **94**, 9138 (1989).
4 For a review of imaging radar satellites, see *Proc. IEEE* **79**, 6 (1991).

Closing in on SH2 Specificity

Raymond B. Birge and Hidesaburo Hanafusa

SH2 (Src homology 2) motifs in certain cytoplasmic proteins are crucial in the signaling pathways of the tyrosine kinase growth factor receptors (*1*, *2*). SH2 domains are 100–amino acid stretches of protein that bind to other proteins containing phosphotyrosine. Short, conserved motifs, primarily three to four amino acids on the carboxyl-terminal side of a phosphotyrosine residue, may actually carry the sequence-specific information for SH2 recognition. The mechanisms behind this specificity are now being unraveled.

Evidence of sequence specificity outside the phosphotyrosine was first inferred from the observation that not all tyrosine kinase receptors (which autophosphorylate on tyrosine residues) bound the same SH2-containing proteins (*3*). Subsequently, small phosphopeptides derived from the primary structure of the platelet-derived growth factor (PDGF) receptor were shown to interfere with guanine triphosphatase (GTPase)–activating protein (GAP) and p85 [a subunit of phosphatidylinositol (PI) 3-kinase] binding to the kinase insert region of the PDGF receptor (*4*). The motif identified,

The authors are in the Laboratory of Molecular Oncology, Rockefeller University, New York, NY 10021

pY(M,V)XM, for binding of the p85 SH2 domain was then found in the polyoma middle T protein (*3*) and later in insulin receptor substrate–1 (IRS-1), where they are also high-affinity binding sites for the SH2 domain of p85 (*5*). The conservation of amino acids on the carboxyl side of the phosphotyrosine suggested that this region carried the sequence-specific information for SH2 recognition. To generalize this premise to other SH2-containing domains, Cantley and colleagues affinity-selected phosphopeptides that bind a particular SH2 domain, starting from a mixture of phosphopeptides that are degenerate from positions +1 to +3 relative to the phosphotyrosine (*6*). Thirteen SH2 domains were tested and, with the exception of the Src family members (Src, Lck, Fyn, and Fgr), each SH2 domain selected a unique motif, and all three degenerative positions contributed to specificity in one case or another. For the SH2 domain of p85, the consensus sequence determined by this method (pYMXM or pYVXM) perfectly matched the true binding sites in the PDGF receptor and polyoma middle T antigen. This approach can be used to characterize the targets of proteins like Crk and Nck for which associating proteins are still unknown, as well as to rationally design phosphopeptides to block upstream SH2 targets.

High-resolution crystallographic analysis of the SH2 domain of Src complexed to small phosphopeptides also reveals the structural criteria for binding specificity. The structure of the Src SH2 domain has been determined with a low- (millimolar) (*7*) and high- (nanomolar) (*8*) affinity phosphopeptide, and the differences are instructive. There are four basic residues at the phosphotyrosine binding site (Arg^{155}, Arg^{175}, His^{201}, and Lys^{203}). Arg^{155}, which is strictly conserved in all SH2 domains except protein tyrosine phosphatase 1C, forms two tight hydrogen bonds with two oxygen atoms of the phosphate. However, unexpectedly, two of the other basic residues interact with the ring system of the tyrosine through amino-aromatic interactions, presumably accounting for the high specificity for phosphotyrosine. Two other SH2 structures have been determined by nuclear magnetic resonance (NMR) in solution and in the absence of peptide [the p85 SH2 domain (*9*) and the SH2 domain of c-Abl (*10*)]. The three SH2 structures known so far span the range of SH2 sequences in terms of three-dimensional structural variation, as shown by a structure-based sequence alignment [see (*7*), in which the p85 SH2 domain is considered to be least similar to the Src SH2 domain], suggesting that variations in overall folding are likely to be minor. Thus, specificity determination must lie mainly in the binding

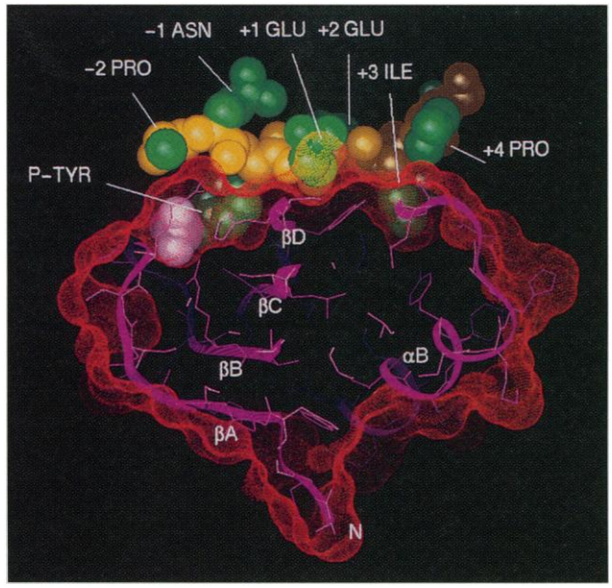

The structure of the SH2 domain of Src. (Upper) Molecular cross section of the Src-SH2 domain complexed to a high-affinity phosphopeptide. Red, the accessible surface; purple, the polypeptide backbone. The phosphopeptide backbone (yellow) and side chains (green) are shown as a space-filling model. White, the phosphate. [Reprinted with permission © from *Cell* Press (*8*)]. **(Lower)** Residues in the Src SH2 domain that contact phosphotyrosine and unique peptide sequences. (●) Amino acids that contact the phosphotyrosine directly and (△) amino acids that contact the high-affinity peptide at positions +1 to +3 relative to the phosphotyrosine. [Adapted from (*8*) and (*11*)]

```
            βA          αA                  βB          βC
GAPN        WYH-GKLD-----RTIAEERL-RQAGKSG------SYLIRES-DRRP-G-SFVLSFLS-QTN-----
PLCγ1N      WFH-GKLGAGRDGRHIAERLL-TEYCIETGAPDG-SFLVRES-ETFV-G-DYTLSFWR-NG------
p85αN       WYW-GDIS-----REEVNEKL-RDTADG-------TFLVRDA-STKMHG-DYTLTLRK-GG------
Lck         WFF-KNLS-----RKDAERQL-LAPGNTHG-----SFLIRES-ESTA-G-SFSLSVRD-FDQNQGE-

                        155                 175
Src         WYF-GKIT-----RRESERLL-LNPENPRG-----TFLVRES-ETTK-G-AYCLSVSD-FDNAKGL-
                           ●                    ● ●

            βD    βD'       βE     βF   αB                    βG
GAPN        VVNHFRI-IAM-C--G---DYYI-GG--RRFS-SLSDLIGYYSHV--SCLLKGEK---LL-YPV
PLCγ1N      KVQHCRI-HSR-QDAGTP-KFFL-TDN-LVFD-SLYDLITHYQQV---PLRCNEFEMRLS-EPV
p85αN       NNKLIKI-FHR-D--G---KYGF-SDP-LTFN-SVVELINHYRNE---SLAQYNPK--LD-VKL
Lck         VIKHYKI-RNL-DN-G---GFYI-SPR-ITFP-GLHDLVRHYTNA-SDGLCTK-----LS-RPC

              201 203
Src         NVKHYKI-RKL-DS-G---GFYI-TSR-TQFS-SLQQLVAYYSKH-ADGLCHR-----LT-NVC
            △●△●                  △ △              △          △△
```

pocket, and indeed crystallographic structure of c-Src (*8*) and Lck (*11*) complexed to a high-affinity phosphopeptide reveal tight docking of side chains at the +1 to +3 positions relative to the phosphotyrosine (see figure, upper part), as was predicted by the biochemical studies. This contrasts with c-Src complexed to a low-affinity phosphopeptide (*7*), in which only the phosphotyrosine moiety makes significant contact with the SH2 platform and the peptide chain is extended away from the surface of the SH2 domain. Interestingly, a comparison of the amino acids in the Src or Lck SH2 domain that directly contact the phosphotyrosine (a general feature of all SH2 domains) to those that contact the +1 to +3 flanking residues in the high-affinity phosphopeptide (specific for Src and Lck SH2) indicates that the most conserved residues in all SH2 domains are those that make direct contact, while the nonconserved residues mainly contact the unique flanking residues (see figure, lower part). The fact that the SH2-containing proteins GAP, p85, PLC-γ, and Src family members recognize unique phosphopeptide motifs in the β-PDGF receptor (Table 1) should make it possible to cocrystallize other SH2 domains with their high-affinity phosphopeptides and further map the molecular basis of SH2 domain–phosphopeptide specificity.

Functionally, this information on binding specificity raises several issues. First, are short phosphopeptides representative of the total phosphoprotein in mimicking biological activity? Studies with the SH2 domain of p85 suggest that certain phosphopeptides can represent the whole protein: Phosphopeptides deduced from the regions of polyoma middle T antigen or PDGF receptor that bind to PI 3-kinase can activate PI 3-kinase in vitro (*12, 13*). This is the first demonstration of activation of an enzymatic activity by the binding of a phosphopeptide to an SH2 domain; it will be of interest to see whether this principle applies to other systems such as Ras activation by Grb2.

Do these findings open a Pandora's box that complicates the use of phosphopep-

Phosphopeptide flanking sequences			
Phosphopeptide	**Residue in PDGF receptor**	**SH2-containing protein**	**Reference**
pYNAPY	(Y^{739})	GAP	(*4*)
pYIIPY	(Y^{1021})	PLC-γ	(*20*)
pYMDMS, pYVPML	(Y^{708}, Y^{719})	p85	(*4*)
pYIYVD	(Y^{579})	Src family kinases	(*21*)

Table 1. Phosphopeptide flanking sequences in the β-PDGF receptor that bind unique SH2 domains. PLC-γ, phospholipase-γ. A, Ala; D, Asp; I, Ile; L, Leu; M, Met; N, Asn; P, Pro; S, Ser; V, Val; Y, Tyr

Mammalian proteins that bind to SH3 domains.		
SH3-containing protein	**Target binding protein**	**Reference**
Grb2	SOS (guanine nucleotide exchange factor)	(*18*)
Abl	3BP-1, 3BP-2 (GAP-like molecule)	(*17*)
Src	PI 3-kinase, cytoskeletal proteins (p110, paxillin)	(*19, 22*)
Crk	C3G (guanine nucleotide exchange factor); c-Abl	(*23*)
Nck	Serine/threonine protein kinase	(*24*)
PLC-γ	Cytoskeletal proteins	(*25*)

Table 2. Some mammalian proteins that bind to SH3 domains.

tides for blocking signaling cascades originating from SH2 binding? The answer may again lie in the phosphotyrosine-SH2 binding affinity and, in particular, how a low-affinity interaction relates functionally to a tighter interaction in its ability to transmit information. Although the sequences immediately adjacent to phosphotyrosine are the primary criteria for SH2 specificity, sequences outside this core sequence may also be important in determining overall affinity, because increasing the phosphopeptide length also increases the affinity (*14*). Binding affinity may also be modulated by covalent modification of the SH2 domain itself (for example, by tyrosine phosphorylation) (*15*).

This is not to say that a higher affinity interaction is always desirable. One can theoretically envision that a low-affinity interaction may be essential under conditions where the local protein concentration is high or where dissociation must occur quickly. For example, the affinity of the Src SH2 domain for a phosphopeptide corresponding to the carboxyl-terminal residue of c-Src (*16*) (an intramolecular interaction thought to inhibit c-Src kinase activity) is approximately 100 times lower than that of a YEEI-containing phosphopeptide selected to be an optimal Src SH2 phosphopeptide from a mixture of degenerate phosphopeptides (*6*).

One can test this by replacing the carboxyl-terminal residue 527 to create a higher affinity motif to examine the effect on c-Src activity. Finally, we need to learn more about the mechanism of SH2-phosphotyrosine disassembly and, in particular, whether this requires enzymatic catalysis.

Many cytosolic signaling proteins that contain an SH2 domain also contain an adjacent SH3 domain, but are SH2 and SH3 domains allosterically coupled within a single molecule? Like SH2 domains, SH3 domains are modular domains that appear to be responsible for assembly of protein-protein complexes. Using an expression-cloning strategy with the Abl SH3 domain, Baltimore and co-workers identified the first SH3 binding protein, called SH3 binding protein–1 (3BP-1) and further characterized a short proline-rich motif, PXXPPPYXP, that appears to be sufficient for SH3 binding to 3BP-1 (*17*). Although the proline-rich sequences probably reflect the core recognition domain, the exact motif that confers specificity in different SH3 domains has not been determined. Recently, many SH3 binding proteins have been cloned (Table 2), revealing that SH3 binding proteins are as functionally diverse as the proteins that contain SH2 and SH3. But how might SH2 and SH3 domains synergize within a single molecule? The most likely way this could occur is for each domain to simultaneously recruit a specific protein into a ternary complex such that the two or more signaling proteins converge to transmit a productive signal. In the case of Grb2, for example, the SH3-dependent Grb2-SOS complex appears to be present in the cytosol of unstimulated cells as an inactive complex. Upon stimulation, the SH2 domain of Grb2 binds the epidermal growth factor (EGF) receptor to allow SOS to translocate and activate Ras proteins at the plasma membrane (*18*). Binding to the receptor may induce a conformational change in the SH3 domain and ensure a directional flow of information from the receptor to the nucleus. Similarly, the SH3 domain of v-Src binds to several proteins of the cortical actin cytoskeleton, including p110 and paxillin (*19*), and this may well explain why v-Src in turn phosphorylates and binds, via its SH2 domain, to these focal adhesion proteins. Indeed, it will be interesting to examine the crystal structure of a tandem SH2-SH3 domain (complexed in the presence and absence of high-affinity peptides) to investigate the potential for cross-talk between these important modular domains.

References and Notes

1. B. J Mayer and D. Baltimore, *Trends Cell Biol.* **3**, 8 (1993).
2. T. Pawson and G. D. Gish, *Cell* **71**, 359 (1992).
3. L Cantley *et al*, *ibid.* **64**, 281 (1991).
4. W. Fanatl *et al.*, *ibid.* **69**, 413 (1992)
5. X J. Sun *et al.*, *Nature* **352**, 73 (1991).
6. Z. Songyang *et al.*, *Cell* **72**, 767 (1993).
7 G. Waksman *et al.*, *Nature* **358**, 646 (1992).
8. G. Waksman, S. E. Shoelson, N. Pant, D. Cowburn, J. Kuriyan, *Cell* **72**, 779 (1993).
9 G. W Booker *et al.*, *Nature* **358**, 684 (1992).
10. M Overduin, C Rios, B. J. Mayer, D. Baltimore, D Cowburn, *Cell* **70**, 697 (1992).
11. M J. Eck, S E Shoelson, S C. Harrison, *Nature* **362**, 87 (1993).
12. J. M Backer *et al*, *EMBO J* **11**, 3469 (1992).
13. C. L Carpenter *et al.*, *J. Biol Chem.* **268**, 9478 (1993).
14. G Panayotou *et al.*, *Mol Cell. Biol.* **13**, 3567 (1993)
15. J. A. Excobedo *et al.*, *ibid.* **11**, 1125 (1991).
16 R. R. Roussel, S. R Brodeur, D Shalloway, A. Laudano, *Proc. Natl. Acad. Sci. U.S.A.* **88**, 10696 (1991).
17. P Cicchetti, B J. Mayer, G. Thiel, D Baltimore, *Science* **257**, 803 (1992); R. Ren, B J Mayer, P Cicchetti, D. Baltimore, *ibid.* **259**, 1157 (1993).
18. S E. Egan *et al.*, *Nature* **363**, 45 (1993); M Rozakis-Adcock *et al.*, *ibid*, p. 83; N. Li *et al.*, *ibid.*, p. 85; N W. Gale *et al*, *ibid.*, p 88
19. Z Weng *et al*, *J. Biol. Chem.* **268**, 14956 (1993).
20 A Kashishian and J. A Cooper, *Mol Cell. Biol.* **4**, 49 (1993).
21. S Mori *et al*, *EMBO J.* **12**, 2257 (1993)
22. Y. Liu, L. E. M Marehgere, C A Koch, T Pawson, *Mol. Cell. Biol.* **13**, 5225 (1993).
23 M Tanaka and M. Matsuda, personal communication; S Feller and H. Hanafusa, unpublished data, R. Ren, Z. S Ye, D. Baltimore, personal communication.
24. M. Chou and H. Hanafusa, unpublished data
25. D. Bar-Sagi *et al.*, *Cell* **74**, 83 (1993)